Optimization and Basis-Set Dependence of a Restricted-Open-Shell Form of B2-PLYP Double-Hybrid Density Functional Theory

David C. Graham,[†] Ambili S. Menon,[†] Lars Goerigk,[†,§,‡] Stefan Grimme,[‡] and Leo Radom*[,†]

School of Chemistry and ARC Center of Excellence for Free Radical Chemistry and Biotechnology, University of Sydney, Sydney, NSW 2006, Australia, NRW Graduate School of Chemistry, Wilhelm-Klemm-Strasse 10, D-48149 Münster, Germany, and Theoretische Organische Chemie, Organisch-Chemisches Institut der Universität Münster, Corrensstrasse 40, D-48149 Münster, Germany

Received: May 8, 2009

The performance of the restricted-open-shell form of the double-hybrid density functional theory (DHDFT) B2-PLYP procedure has been compared with that of its unrestricted counterpart using the G3/05 test set. Additionally, the influence of basis set on the parametrization and performance of ROB2-PLYP, and the further improvement of ROB2-PLYP through augmentation with a long-range dispersion function, have been investigated. We find that, after optimization of the two empirical DHDFT parameters, the ROB2-PLYP method (HF exchange = 59% and MP2 correlation = 28%) performs slightly better than the corresponding UB2-PLYP method (HF exchange = 62% and MP2 correlation = 35%), with mean absolute deviations (MADs) from the experimental energies in the G3/05 test set of 9.1 and 9.9 kJ mol^{-1}, respectively, when the cc-pVQZ basis set is employed. Separate optimizations of the parameters for the RO and U procedures are crucial for a fair comparison. For example, for the G2/97 test set, ROB2-PLYP(53,27) and ROB2-PLYP(62,35) show MADs of 12.2 and 13.5 kJ mol^{-1}, respectively, compared with the 6.6 kJ mol^{-1} for (the optimized) ROB2-PLYP(59,28). The performance of ROB2-PLYP deteriorates significantly as the basis-set size is decreased, reflecting the enhanced basis-set dependence of the MP2 contribution compared with standard DFT. We find that this deficiency can be partly overcome through reparametrization. However, when the basis set drops below triple-ζ, the improvements made on reoptimizing the ROB2-PLYP parameters are not sufficient to warrant their general use. We find that the dispersion- and BSSE-corrected ROB2-PLYP(59,28)-D HCP procedure performs significantly better than ROB2-PLYP(59,28) for the S22 test set of interaction energies in which dispersion interactions are particularly important, with the MAD falling from 6.1 to 1.6 kJ mol^{-1}. However, when the same D correction is applied to the G3/05 test set, the performance of ROB2-PLYP(59,28)-D deteriorates slightly compared with ROB2-PLYP(59,28), with the MAD increasing from 9.1 to 9.5 kJ mol^{-1}.

1. Introduction

The development of highly accurate quantum chemical methods that can reliably predict thermochemical data when experimental data are unavailable or uncertain is highly desirable. High-level composite procedures, such as the G*n*(X) methods of Curtiss, Raghavachari, and Pople et al.,[1] the complete-basis-set (CBS) methods of Petersson et al.,[2] and the W*n* methods of Martin et al.,[3] have made the task of achieving chemical accuracy—for small systems at least—very feasible. However, as a consequence of their cost, calculations on systems larger than those containing a few non-hydrogen atoms are typically out of reach with these methods.[4] Thus it may be necessary to sacrifice both accuracy and the capacity for systematic improvement to work on systems that are more chemically relevant.[5]

Density functional theory (DFT) provides an alternative method for the calculation of accurate energies, at a cost comparable to that of Hartree−Fock calculations.[6] Although DFT methods do not offer a systematic way to improve the Hamiltonian,[5] Perdew et al.[7] have put forward a "Jacob's Ladder" analogy for improving the critical exchange−correlation component of DFT functionals. In this strategy, each higher rung on the ladder is expected to offer an additional improvement in the accuracy over the basic (bottom rung) local density approximation (LDA) approach.

Grimme has recently proposed a new family of methods,[4,8,9] termed "double-hybrid" density functional theory (DHDFT) procedures, that are consistent with a fifth rung approach in the "Jacob's Ladder" of DFT methods. These procedures not only incorporate Hartree−Fock exchange admixture in the same way that hybrid DFT procedures such as the immensely popular B3-LYP[10] do but also combine contributions from the semilocal correlation density functional with a proportion of MP2 correlation derived using the Kohn−Sham (KS) reference orbitals (KS-PT2).[11] The DHDFT energy is obtained by first solving the KS equations self-consistently using a hybrid density functional containing a semilocal generalized gradient approximation (GGA) for exchange (X) and correlation (C). Second, the MP2 energy (E2) is calculated in the space of the converged KS orbitals. The total exchange−correlation energy for the DHDFT procedure is then obtained by summation of the various parts of the functional:[4]

$$E_{XC}^{DHDFT} = (1 - a_X)E_X^{DFT} + a_X E_X^{HF} + (1 - a_C)E_C^{DFT} + a_C E2 \quad (1)$$

where E_X is the exchange energy and E_C is the correlation energy. The Møller−Plesset perturbation correction term (E2) is given by

[†] University of Sydney.
[‡] Universität Münster.
[§] NRW Graduate School of Chemistry.

10.1021/jp9042864 CCC: $40.75 © 2009 American Chemical Society
Published on Web 07/31/2009

$$E2 = \frac{1}{2}\sum_{ia}\sum_{jb}\frac{(ia|jb)[(ia|jb) - (ib|ja)]}{\varepsilon_i + \varepsilon_j - \varepsilon_a - \varepsilon_b} \quad (2)$$

where the ε_i are the Kohn−Sham orbital energies obtained from the self-consistent solution of the hybrid GGA part of the method. As MP2 scales with the fifth power of system size, the main advantage in choosing DFT as a high-accuracy but low-cost method may appear partly lost.[12] However, the additional expense of the MP2 portion of the DHDFT calculation can be circumvented somewhat through the use of the resolution-of-the-identity approximation (RI)[13] where a speed-up of 3−15 times[14] can be obtained with less than 0.1 kJ mol^{-1} atom^{-1} loss in accuracy when calculating relative energies.[4] Alternative approaches that have been utilized to decrease the expense of the MP2 portion in DHDFT calculations include opposite-spin (OS) MP2[15] and frozen-core MP2.[12]

In principle, any density functional theory method can be used for the calculation of the GGA exchange and correlation.[8] Grimme's initial DHDFT procedure[8] was based on standard GGAs for exchange (X) due to Becke (B88)[10a,b] and for correlation (C) due to Lee, Yang, and Parr (LYP).[10c] This method, termed B2-PLYP because of its two empirical parameters and its second-order perturbative contribution to the correlation, derived the required constants for HF exchange ($a_X = 53\%$) and MP2 correlation (E2) ($a_C = 27\%$) through a least-squares-fit to the G2/97 set of 148 reliable experimental values of heats of formation. The development of mPW2-PLYP followed subsequently,[9] and utilized the modified Perdew−Wang exchange functional (mPW)[16] in preference to that of Becke (B88), with the aim of providing an improvement associated with the superior performance of mPW exchange in low-density regions.[9] However, the optimized constants for mPW2-PLYP (i.e., $a_X = 55\%$ and $a_C = 25\%$) were derived through minimizing the mean absolute deviation (MAD) of a 23 molecule subset from the G2/97 heat of formation set. The mPW2-PLYP method has received relatively less attention when compared with B2-PLYP.

The performance of the X2-PLYP (X = B or mPW) DHDFT procedures has been remarkable when compared with conventional hybrid DFT methods in the calculation of reaction energies from standard test sets.[4,8,9,12] Both B2-PLYP and mPW2-PLYP have yielded the smallest mean absolute deviations (MADs) ever obtained by a density functional theory method for the full G3/05 test set (10.5 and 8.8 kJ mol^{-1}, respectively), in combination with a big improvement in the maximum errors.[9] In comparison, the related pure (B-LYP) and hybrid (B3-LYP) DFT procedures exhibit MADs of 31.0 and 18.4 kJ mol^{-1}, respectively, for the G3/05 test set.[9]

Other encouraging results with the X2-PLYP methods have been achieved for radical stabilization energies,[17] isomerization energies,[4,14] excited states,[18] electronic circular dichroism spectra,[19] transition metal reactions,[20] and kinetics.[12] The development of analytical gradients has extended the applicability of these new DHDFT procedures to potential energy surfaces, where they have shown performance superior to isolated DFT and MP2 methods, with an accuracy approaching that of CCSD(T), albeit with a significant increase in computational cost.[21]

Martin et al. have recently carried out a comprehensive study in which they have reparametrized both B2-PLYP and mPW2-PLYP using a variety of test sets in an attempt to obtain performance superior to that of the original X2-PLYP methods for a range of thermodynamic and kinetic properties.[12] This has resulted in new methods that are optimized for kinetics (B2K-PLYP, $a_X = 72\%$, $a_C = 42\%$; mPW2K-PLYP(72,42)), thermochemistry (B2T-PLYP(60,31)), and a compromise method suitable for general purpose applications (B2GP-PLYP(65,35)).[12] The optimum parameters for the double-hybrids for individual data sets representing hydrogen-transfer reactions, heavy-atom transfers, nucleophilic substitutions, and unimolecular and recombination reactions were found to show significant variation.[12]

The superior performance of the DHDFT procedures is believed to stem from a "marriage of convenience" between the DFT and MP2 parts of the functional.[12] DFT handles the short-range correlation[12] and provides a more stable reference for the calculation of the MP2 energy,[4] while the MP2 contribution provides the benefit of including nonlocal dynamical electron correlation responsible for long-range interactions.[8,9] However, the price to pay for this combination is that the new method may inherit some of the undesirable traits inherent to either MP2 or DFT.

For example, the X2-PLYP methods are expected to show slower basis-set convergence than standard DFT procedures due to their MP2 component. This suggests the need for much larger basis sets than those that would be typically employed for DFT calculations.[12] Grimme has suggested[8] that the basis-set dependence of B2-PLYP should lie between that of standard DFT and MP2 and that reliable results are usually obtained with a properly polarized triple-ζ basis set.[8] Martin et al. have tested the "general purpose" B2GP-PLYP procedure for the W4-08 data set using a variety of basis sets of triple-ζ quality or better.[12] Mean absolute deviations were found to range from 5.9 kJ mol^{-1} (apc4, 5Z quality) to 18.2 kJ mol^{-1} (MG3S, TZ quality), although the extrapolated core−valence triple-ζ basis set aug-cc-pwCVTZ also performed well (7.5 kJ mol^{-1}).[12] Interestingly, the performance of standard B2-PLYP on the W3 atomization energies data set was found to *deteriorate* for basis sets larger than triple-ζ, whereas the performance of the double-hybrid kinetics method (B2K-PLYP) improved with increasing basis set size.[12] It has been suggested[12] that reparametrization of DHDFT procedures to remedy the decline in the MP2 contribution caused by smaller basis sets would result in an exaggerated MP2 admixture coefficient to compensate. However, exactly how much of this basis set deficiency can be overcome through reparametrization has not previously been assessed systematically.

Also of concern is whether or not DHDFT procedures are subject to the same types of problems as UMP2 when open-shell systems are considered. Specifically, selection of a spin-contaminated reference function can lead to chronic errors when performing a subsequent UMP2 calculation, and it is therefore preferable to start from a reference function that does not suffer from problems of spin contamination.[22] As a consequence, a restricted Hartree−Fock (ROHF) reference is often employed for MP2 calculations in such situations (i.e., ROMP2), resulting in a substantial improvement for predicted energies.[17,22] In this connection, many of the popular composite methods have also been specifically adapted to use the non-spin-contaminated restricted HF reference functions for open-shell systems. This has given rise to method extensions such as G3X-RAD,[23] CBS-RAD,[24] and ROCBS-QB3.[25] Although the consequences of spin contamination in the KS orbitals on the resulting DFT energies are not definitively known, there are strong indications that DFT densities and energies are less affected by spin contamination than are the corresponding unrestricted Hartree−Fock quantities.[26] However, both the method used to calculate the level of spin-contamination (e.g., deviation in $\langle S^2 \rangle$ from the value corresponding to a pure spin state) and whether or not the

level of spin contamination in the KS orbitals is even relevant are still subjects of discussion.[5,26−29] In practice, the use of the unrestricted KS orbitals as a reference for higher-level wave function methods such as MP2,[11] CC,[30] and CI[31] has proved advantageous over the more common UHF reference, but it is still not without problems.[32]

While the basis for the use of restricted-open-shell KS (ROKS) orbitals in an attempt to remove spin contamination has been questioned,[27] in many cases ROKS-DFT has shown equal or improved performance when compared with its UKS counterpart.[26,33] Using the HF exchange and E2 parameters optimized for (U)B2-PLYP (i.e., 53,27) and (U)mPW2-PLYP (i.e., 55,25), the performance of these ROX2-PLYP methods has recently been trialled for the calculation of bond dissociation energies (BDEs) and radical stabilization energies (RSEs) for a test set of 22 monosubstituted methyl radicals.[17] In this investigation, the restricted versions of the DHDFT procedure clearly performed better than their unrestricted counterparts for BDEs, while both restricted and unrestricted forms of the DHDFT procedures exhibited the best performance of all the hybrid DFT methods surveyed with regard to RSEs. This was despite the fact that the X2-PLYP procedures had been optimized for the U-DHDFT rather than RO-DHDFT procedure. In a more recent study,[29] the same test set of 22 homolytic bond dissociation reactions was used to assess the susceptibility of various DFT methods to spin contamination. The influence of spin contamination on unrestricted DHDFT procedures was found to be among the lowest of all the methods surveyed due to the opposing behavior of the UHF and UMP2 components with respect to spin contamination. This resulted in differences between U-DHDFT and RO−DHDFT procedures that were typically less than 5 kJ mol^{-1}, compared with U/RO differences of up to 70 kJ mol^{-1} for HF and 96 kJ mol^{-1} for MP2. Though the test set was reasonably small, these results suggest that, while the performance for BDEs of the restricted form of DHDFT is generally superior, spin contamination is only of minimal concern for unrestricted DHDFT.

The underestimation of long-range dispersion forces has been described as the only known shortcoming of DHDFT.[34] While the incorporation of an MP2 component into the functional mitigates this inherent shortcoming somewhat, the fractional addition of MP2 correlation in the current DHDFT procedures is unable to cope with the full extent of the problem,[4,12,34] resulting in vdW complexes that are under-bound.[8] This deficiency has been diminished through incorporation of an empirical add-on damped dispersion function[35] to DHDFT.[34] When the dispersion-incorporated B2-PLYP-D method was used, the mean absolute deviation (MAD) for the G3/99 heat of formation set was found to improve from 10.0 kJ mol^{-1} with B2-PLYP to just 7.1 kJ mol^{-1}.[34] The amount of dispersion added is scaled depending on which DHDF procedure it is being added to, with a linear relationship found to exist between the dispersion scaling factor (s_6) and the amount of MP2 correlation included in the DHDFT.[12]

Following on from our earlier assessment of the performance of the unoptimized ROB2-PLYP method for the calculation of RSEs and BDEs,[17] we present here a full assessment of reparametrized versions of the ROB2-PLYP method for the 455 energies in the G3/05 test set. We also aim to establish the sensitivity of the method toward basis-set size (especially small basis sets) and look at its further improvement through augmentation with a long-range dispersion function.

2. Theoretical Procedures

Geometry optimizations were carried out at the UB3-LYP[10] level using a double-polarized triple-ζ-valence basis set[36] (TZV2P), with the polarization functions taken from the cc-pVTZ basis set[37] with the highest angular momentum function discarded. Zero-point vibrational energies (ZPVEs) and thermal corrections to the enthalpy were obtained at the same level of theory as the geometry optimizations. Scale factors for this level have been recently determined as 0.9873 for the ZPVE and 1.0058 for the thermal correction.[38] Subsequent B2-PLYP[8] single-point calculations were performed with the standard cc-pVQZ, cc-pVTZ, cc-pVDZ, 6-311+G(3df,2p), 6-31+G(2d,p), and 6-31G(d) basis sets. The CQZV basis set of Feller and Peterson[39] was used for potassium in calculations that used the Dunning cc-pV*n*Z basis sets for the other elements. For the calculation of electron affinities (EA) and hydrogen-bond energies (HB), additional diffuse functions were used,[1,40] with the aug-cc-pVQZ, aug-cc-pVTZ, aug-cc-pVDZ, 6-311++G-(3df,2p), 6-31++G(2d,p), and 6-31+G(d) basis sets, respectively, replacing those basis sets described previously. For comparison purposes, calculations were also performed using the pure (B-LYP) and hybrid (B3-LYP) DFT methods.

Calculations were carried out for the 148 molecules in the G2/97 heats of formation test set[41] and the complete G3/05 test set.[42] The G3/05 test set comprises 271 heats of formation, 105 ionization energies, 63 electron affinities, 10 proton affinities, and 6 hydrogen-bond energies, all of which were selected on the basis of their small quoted experimental uncertainties. Reference experimental data were taken from various sources.[1,41−43]

The calculated molecular energies were used to derive heats of formation at 298 K ($\Delta_f H_{298}$) using the atomization procedure outlined by Nicolaides et al.[44] (the calculated atomization energy being subtracted from the experimental heats of formation of the atoms). Experimental thermal corrections were obtained from ref 41. Where stated, spin−orbit coupling corrections obtained from refs 1e and 1f were applied to atoms with ^{2}P and ^{3}P electronic states. No spin−orbit corrections were applied to molecules. The other results (i.e., ionization energies, electron affinities, proton affinities and hydrogen-bond energies) refer to enthalpies at 0 K with scaled ZPVE corrections.

For the weakly bonded complexes in the S22 test set of Hobza,[45] geometries were used as supplied, and interaction energies were corrected for basis set superposition error (BSSE) using standard counterpoise methods.[46] Where indicated, an empirical dispersion correction method was used on the basis of damped, atom-pairwise $-C_6R^{-6}$ potentials (DFT-D),[35] with the total energy given by

$$E_{\mathrm{DHDFT-D}} = E_{\mathrm{DHDFT}} + E_{\mathrm{disp}} \tag{3}$$

where E_{DHDFT} is the conventional double-hybrid density functional theory energy and E_{disp} is an empirical dispersion correction given by

$$E_{\mathrm{disp}} = -s_6 \sum_{i=1}^{N_{\mathrm{at}}-1} \sum_{j=i=1}^{N_{\mathrm{at}}} \frac{C_6^{ij}}{R_{ij}^{\ 6}} f_{\mathrm{dmp}}(R_{ij}) \tag{4}$$

where N_{at} is the number of atoms in the system, C_6^{ij} denotes the dispersion coefficient from atom pair "*ij*" (obtained from ref 35b), s_6 is a global scaling factor that only depends on the functional used and R_{ij} is an interatomic distance. A damping

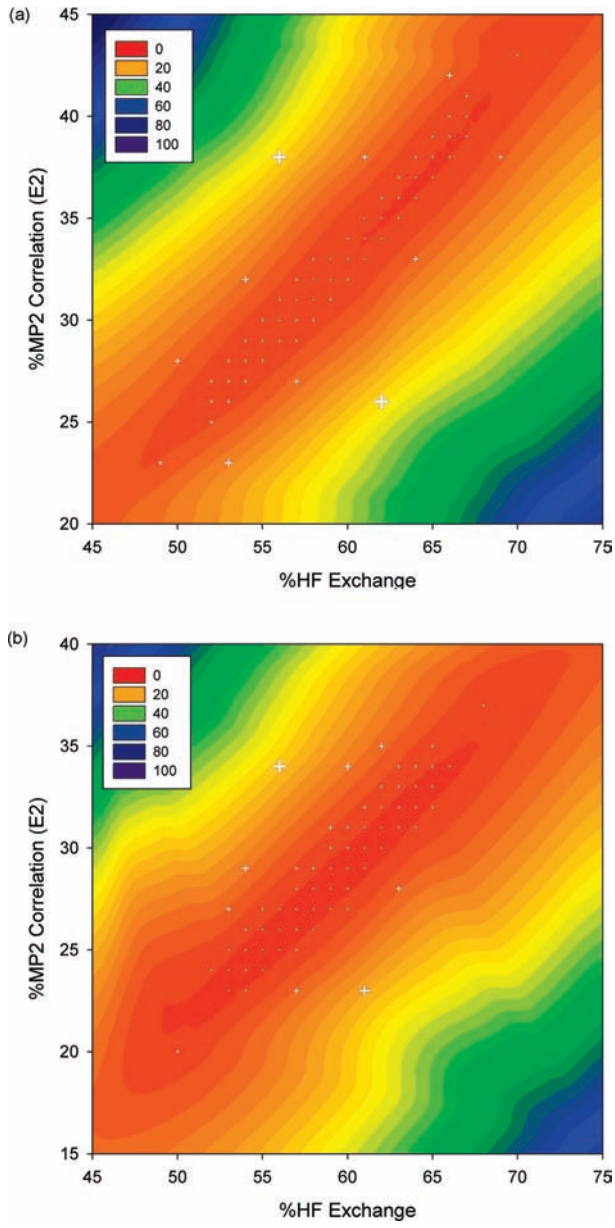

Figure 1. Changes in the mean absolute deviation (MAD, kJ mol^{-1}) from experiment for the G2-97 heats of formation test set with respect to the percentage of Hartree−Fock exchange and MP2 correlation included in the (a) UB2-PLYP(X,C) and (b) ROB2-PLYP(X,C) methods. All calculations were performed using the cc-pVQZ basis set. Crosses define the data points used to generate the surface, with their size proportional to the MAD at that point.

function f_{dmp} is also used to avoid double counting, for which the details can be found elsewhere.[34]

All calculations were carried out using the Gaussian 03 suite of programs.[47]

3. Results and Discussion

3.1. Parametrization of UB2-PLYP and ROB2-PLYP. Although an assessment of the performance of the (U)B2-PLYP method for the G3/05 test set has already been performed,[9] we have reoptimized and reassessed the UB2-PLYP method with the slightly different prescriptions of the present study to provide a fair assessment of the ROB2-PLYP method when compared with its unrestricted counterpart. We hope in this way to remove any significant differences that may influence the results, other than the change from an unrestricted to a restricted formalism.

The a_X and a_C parameters for both UB2-PLYP and ROB2-PLYP were thus reoptimized by minimizing the mean absolute deviation (MAD) from experimental values for specified benchmarking sets, before the testing of each method for the G3/05 set was carried out. The present calculations used somewhat less complex (and more readily available) basis sets than the original assessment, incorporated recently calculated zero-point energy and thermal correction scaling factors for the chosen model, used standard (non-RI) MP2, and used a different software package (which may have ramifications due to grid-size or convergence cut-offs). To avoid confusion, we use the notation "B2-PLYP" or "(U)B2 PLYP" to refer to the original (standard) B2-PLYP procedure, whereas we use "UB2-PLYP(X,C)" or "ROB2-PLYP(X,C)" to refer to our newly optimized procedures. The parameters X and C refer to the extent of incorporation of HF exchange and MP2 correlation, respectively. For example, ROB2-PLYP(59,28) refers to the restricted-open-shell B2-PLYP procedure with 59% HF exchange and 28% MP2 correlation.

Calculation of heats of formation is believed to be one of the harshest tests of any theoretical method, as it formally deals with multiple bond-breaking processes.[4,6] Akin to the method employed originally for the optimization of the two empirical parameters in (U)B2-PLYP,[8] the 148 heats of formation from the G2/97 test set have been used as the benchmarking data set for parameter optimization. The cc-pVQZ basis set, which is similar in the valence space to the C3PVZ basis set employed by Grimme for his benchmarking studies,[8] has been used for the calculations. However, cc-pVQZ does not include the tight core functions that are incorporated in the C3PVZ basis and which have been very recently described as being an important inclusion for DHDFT calculations.[12]

The changes in mean absolute deviations (MADs) from experiment for UB2-PLYP(X,C) associated with variations in the proportions of HF exchange (a_X) and MP2 correlation (a_C) are displayed in Figure 1a. The shape of the surface is similar to that found in recent studies by Martin et al.[12] when the B2-PLYP parameters were reoptimized for the W3 test set. The

TABLE 1: Influence of the Inclusion of Spin−Orbit Coupling on the Performance of the Parameter-Optimized UB2-PLYP and ROB2-PLYP Methods with the G2/97 Heats of Formation Set[a]

		optimized parameters		G2/97 ΔH_f set performance			
method	SOC[b]	E_X^{HF} (%)	$E2$ (%)	MAD[c]	MD[c]	MAD[d]	MD[d]
UB2-PLYP	N	62	35	7.4	−0.1	8.4	1.9
UB2-PLYP	Y	66	39	8.1	1.6	9.7	4.6
ROB2-PLYP	N	59	28	6.6	1.0	12.2	−10.8
ROB2-PLYP	Y	58	28	7.3	1.3	11.3	−8.1

[a] All energies are in kJ mol^{-1} and were obtained using the cc-pVQZ basis set. [b] Spin−orbit correction is applied to atoms (refer Theoretical Procedures). [c] Mean absolute deviation and mean deviation using the tabulated optimum parameters. [d] Mean absolute deviation and mean deviations using the original B2-PLYP parameters (53% HF exchange, 27% MP2 correlation) from ref 8.

TABLE 2: Effect of Changing from UB2-PLYP to ROB2-PLYP on the Mean Absolute Deviation (MAD), and Mean Deviation (MD) from Experiment for Both the G2/97 Heats of Formation Set and the Radicals within the Set[a]

	parameters		G2/97 ΔH_f set performance (radicals)			
method	E_X^{HF} (%)	$E2$ (%)	MAD[b]	MD[b]	(MAD)[c]	(MD)[c]
UB2-PLYP	62	35	7.4	−0.1	5.5	−2.7
ROB2-PLYP	62	35	13.5	−12.2	8.8	−8.0
ROB2-PLYP	59	28	6.6	1.0	4.7	−1.0

[a] All energies are in kJ mol^{-1} and are obtained using the cc-pVQZ basis set. [b] Mean absolute deviations and mean deviations for the G2/97 heats of formation test set (148 molecules). [c] Mean absolute deviations and mean deviations for the open-shell species in the G2/97 heats of formation test set (30 molecules).

surface exhibits a channel that runs diagonally from low to high values of both the HF exchange (a_X) and MP2 (a_C) scaling parameters. Within the channel, the MAD changes slowly, deviating by approximately 1 kJ mol^{-1} from the minimum of 7.4 kJ mol^{-1} (62,35) on moving toward the extremes of the data points shown within the channel. In contrast, however, parameter changes that result in movement perpendicular to the defined channel lead to a rapid increase in MAD, as found previously by Martin et al.[12]

The minimum MAD of 7.4 kJ mol^{-1} is similar to that obtained in an earlier study[9] for the same test set (7.5 kJ mol^{-1}), although the optimized parameters (i.e., 62,35) differ significantly from those found previously (i.e., 53,27).[8] On our surface, the original B2-PLYP parameters correspond to an MAD of 8.4 kJ mol^{-1} and a mean deviation (MD) that skews the distribution toward the right, indicating that B2-PLYP(53,27) is overbound in nature (Table 1). It seems likely that this change in optimum parameters is primarily a consequence of the different basis sets used in the two studies. Interestingly, the optimized parameters for B2T-PLYP (60,31)[12] and B2GP-PLYP (65,36)[12] lie close to the new optimized values obtained in the present study.

The inclusion of an atomic spin−orbit correction (SOC) in the calculated heats of formation shifts the optimum parameters to even higher HF and MP2 values (66,39). More importantly, after applying the SOC, the optimum performance of the method deteriorates slightly, giving an MAD of 8.1 kJ mol^{-1} (Table 1). This result is consistent with findings from a previous study in which eight out of ten DFT procedures showed poorer performance for the G3/05 test set when a spin−orbit correction was applied, with B3-LYP being the most sensitive.[42]

The results for the $E_X^{HF}/E2$ surface obtained using the analogous restricted-open-shell method (ROB2-PLYP) are shown in Figure 1b. Again, the dominant feature on the surface is the optimum MAD channel that runs diagonally from low HF exchange (a_X) and MP2 correlation (a_C) scaling parameters to high a_X and a_C values. Compared with the UB2-PLYP(X,C) surface, the position of the channel on the ROB2-PLYP(X,C) surface is shifted toward lower $E2$ scaling values by between three and eleven percentage points. This shift to lower a_C values is also reflected in the position of the minimum that now lies at 59% HF exchange and 28% MP2 correlation and has an improved MAD of just 6.6 kJ mol^{-1} (Table 1). The inclusion of atomic spin−orbit corrections in the calculation of the heats of formation again causes a slight deterioration in the performance of the method (MAD = 7.3 kJ mol^{-1}) and shifts the optimized parameters very slightly (58,28).

It is important to note that the improvement in performance of B2-PLYP for the G2/97 test set when moving from the unrestricted to the restricted form only occurs after the HF exchange (a_X) and MP2 correlation (a_C) parameters are reoptimized. If the restricted form of the method is used employing parameters optimized for the unrestricted form (i.e., ROB2-PLYP(62,35)) or with the (53,27) parameters of standard B2-PLYP, there is a significant increase in MAD from 6.6 to 13.5

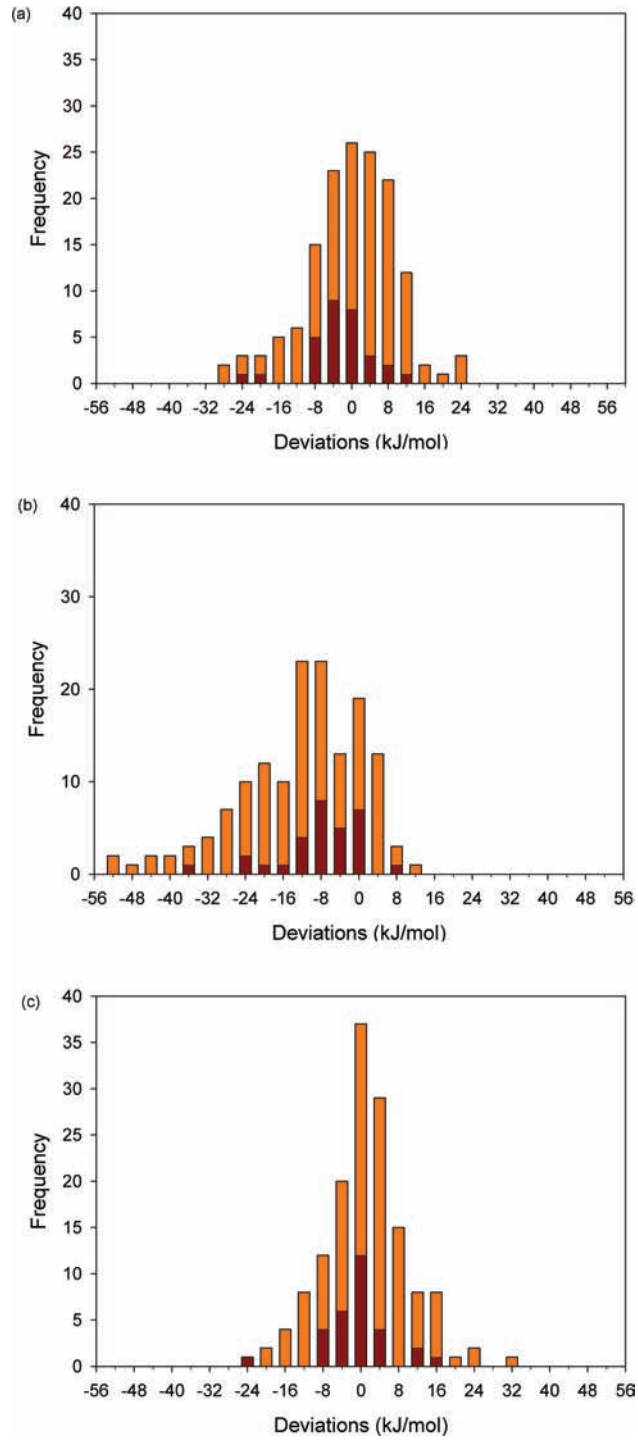

Figure 2. Effect of changing from UB2-PLYP to ROB2-PLYP on the distribution of deviations from experimental values for both the G2/97 heats of formation test set (148 molecules, orange bars) and for the radicals within the set (30 radicals, red bars): (a) UB2-PLYP with optimized parameters (62% HF exchange, 35% MP2 correlation); (b) ROB2-PLYP using UB2-PLYP optimized parameters (62,35); (c) ROB2-PLYP using optimized parameters (59,28). All calculations were performed using the cc-pVQZ basis set. Each vertical bar represents deviations in a 4 kJ mol^{-1} range.

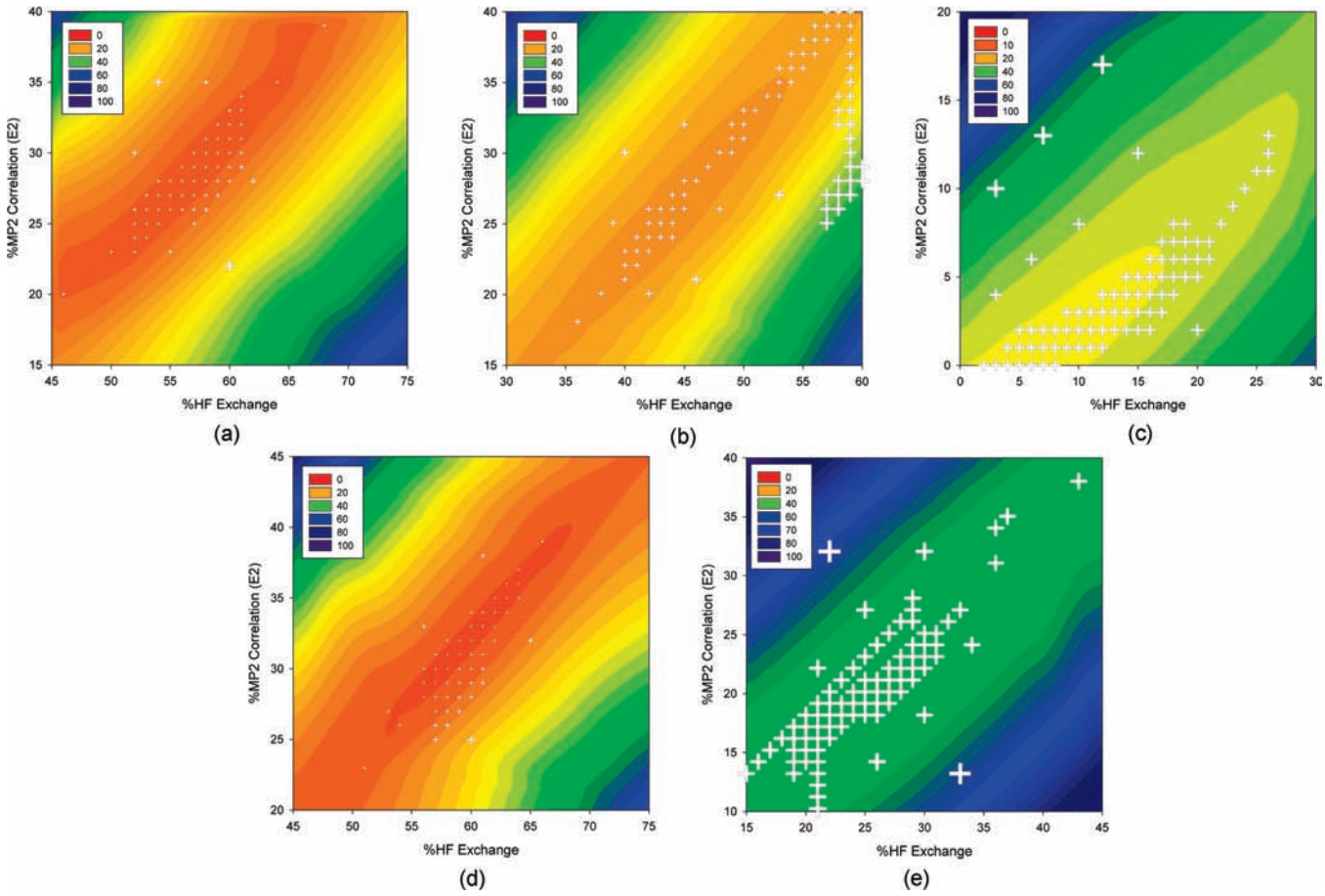

Figure 3. Changes in the mean absolute deviation (MAD, kJ mol^{-1}) from experimental values for the G2/97 heats of formation test set with respect to basis set and the percentage of Hartree−Fock exchange and MP2 correlation included in the ROB2-PLYP(X,C) method. Pople basis sets: (a) 6-311+G(3df,2p); (b) 6-31+G(2d,p); (c) 6-31G(d); Dunning basis sets: (d) cc-pVTZ; (e) cc-pVDZ. Results for cc-pVQZ are included in Figure 1b. Crosses define the data points used to generate the surface, with their size proportional to the MAD at that point.

or 12.2 kJ mol^{-1} (Table 2). Error distribution plots (Figure 2) indicate that the move from the unrestricted (Figure 2a) to the restricted (Figure 2b) B2-PLYP procedure while retaining the optimized UB2-PLYP(62,35) parameters results in a distribution that is skewed markedly to the left (MD = −12.2 kJ mol^{-1}), an indication that the heats of formation are predicted to be much lower than the experimental values (i.e., total atomization energies are too high). This shift is not entirely unexpected as the majority (118 out of 148) of the molecules in the G2/97 heats of formation set are closed-shell species where the difference in heats of formation calculated by the restricted (ROB2-PLYP) and unrestricted (UB2-PLYP) methods arises entirely from differences in the atomic energies since there is no change in the molecular calculations. As the restricted form of B2-PLYP(X,C) predicts the atoms to be higher in energy by between 0.0 and 6.2 kJ mol^{-1}, the general trend is a shift toward lower heats of formation, as observed. A reduction in both the HF exchange and MP2 correlation scaling parameters corrects the skew of the distribution and dramatically improves the MAD (Figure 2c).

A proportion of the overall improvement in MAD on going from UB2-PLYP(62,35) to ROB2-PLYP(59,28) can be attributed to the improvement in the representation of the thirty open-shell species among the 148 species in the G2/97 heats of formation set. The MAD of this radical subset improves by 0.8 kJ mol^{-1} on going from the optimized UB2-PLYP(62,35) to the optimized ROB2-PLYP(59,28) method (Table 2). The ROB2-PLYP(59,28) MAD (4.7 kJ mol^{-1}) lies between that previously calculated for the same set of radicals using the considerably more expensive G3 (3.5 kJ mol^{-1}) and G3(MP2) (5.1 kJ mol^{-1}) methods.[43]

3.2. ROB2-PLYP Basis-Set Dependence. To ascertain the effect of basis-set size on the optimum parameters and performance of ROB2-PLYP(X,C), a total of six basis sets were selected, comprising three Dunning-type (i.e., cc-pVQZ, cc-pVTZ and cc-pVDZ) and three Pople-type (i.e., 6-311+G(3df,2dp), 6-31+G(2d,p) and 6-31G(d)) sets. The $E_X^{HF}/E2$ surfaces (Figure 3) again all exhibit the channel feature described above for the cc-pVQZ basis set (Figure 1b). However, the optimum parameters and MAD values vary dramatically. In increasing MAD order, the basis sets and their associated optimum parameters are cc-pVQZ(59,28) (MAD = 6.6 kJ mol^{-1}), cc-pVTZ(60,32) (MAD = 9.5 kJ mol^{-1}), 6-311+G(3df,2p)(55,27) (MAD = 11.2 kJ mol^{-1}), 6-31+G(2d,p)(53,25) (MAD = 18.8 kJ mol^{-1}), 6-31G(d)(5,0) (MAD = 32.2 kJ mol^{-1}) and cc-pVDZ(28,22) (MAD = 47.2 kJ mol^{-1}) (Table 3). We can see that the performance of ROB2-PLYP deteriorates substantially when the basis set falls below triple-ζ quality, as expected for a well-behaved quantum chemical method. This indicates that the double-hybrid approach suffers less than other functionals from uncontrollable error compensations. This is observed, for example, for B3-PLYP, which seems to perform very well with the relatively small 6-31G(d) basis set but for which the accuracy can deteriorate for larger basis sets. In agreement with this view we find that the poor behavior of ROB2-PLYP for smaller basis sets can be only partly overcome

TABLE 3: Effect of Basis Set on the Optimum ROB2-PLYP Parameters and the Performance of these Methods for the G2/97 Heats of Formation Test Set[a]

	optimized parameters		ROB2PLYP[b]		ROB2PLYP[c]		ROB3LYP		ROBLYP	
basis set	E_X^{HF} (%)	$E2$ (%)	MAD	MD	MAD	MD	MAD	MD	MAD	MD
cc-pVQZ	59	28	6.6	1.0	12.2	−10.8	12.9	−4.4	31.4	−11.0
cc-pVTZ	60	32	9.5	3.6	10.1	0.5	12.8	1.7	31.8	−5.6
cc-pVDZ	28	22	47.2	19.0	75.0	74.9	43.7	41.9	53.2	32.0
6-311+G(3df,2p)	55	27	11.2	3.5	12.1	−1.4	12.8	−4.8	32.2	−10.1
6-31+G(2d,p)	53	25	18.8	7.5	28.1	27.6	16.6	7.4	28.6	1.3
6-31G(d)	5	0	32.2	10.9	59.5	58.5	19.3	11.9	33.6	0.2

[a] All energies are in kJ mol^{-1}. [b] Using optimized parameters from this work. [c] Using the original (U)B2-PLYP parameters (i.e., 53% HF exchange and 27% MP2 correlation) from ref 8.

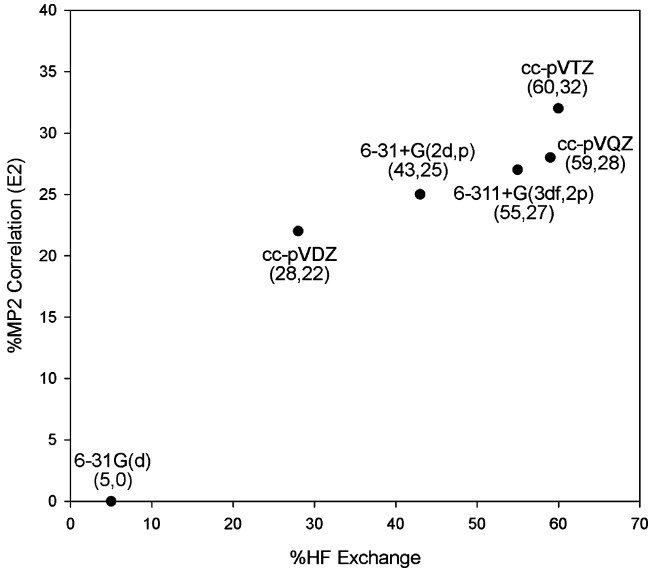

Figure 4. Location of the optimum ROB2-PLYP parameters for each of the six basis sets surveyed.

through reparametrization. Depending on the basis set employed, reoptimization of the a_X and a_C parameters from the (59,28) of the cc-pVQZ basis set provides an improvement of between 0 and 41 kJ mol^{-1} in the MAD for the G2/97 heat of formation set, i.e., without the reoptimizations the results for the smaller basis sets are even worse than those noted in Table 3. A striking result is that, in cases where the basis set has less than triple-ζ quality, the standard ROB3-LYP single-hybrid DFT procedure shows superior performance to the optimized ROB2-PLYP double-hybrid DFT method.

The triple-ζ and larger basis sets (i.e., cc-pVQZ, cc-pVTZ and 6-311+G(3df,2p)) have optimized parameters for ROB2-PLYP(X,C) that are clustered around the region of 55−60% HF exchange and 27−32% MP2 correlation (Figure 4). As the basis set quality decreases below triple-ζ, there is a decrease in both the proportion of HF exchange and MP2 correlation included in the method until finally the optimized parameters for ROB2-PLYP/6-31G(d) result in a method that has no E2 contribution at all!

We have selected three molecules that are representative of the G2/97 heats of formation set, i.e., a homodiatomic (S_2), a heterodiatomic (HCl), and a hydrocarbon (ethane), to illustrate the consequences of decreasing the size of the basis set on the energy components that contribute toward the total atomization energy (TAE), and thus the heat of formation. Using fixed B2-PLYP parameters (62,35), Figure 5 shows the effect that a decrease in size of both the Dunning and Pople basis sets has on results for the three selected prototypical molecules (refer to Supporting Information for tabulated data).[48] The TAE has contributions from the kinetic energy (T), potential energy (V), electron repulsion (J), and nuclear repulsion (N) (expressed collectively as E_{TVJN}), the nonlocal exact HF exchange E_X(HF), the semilocal DFT (B88) exchange E_X(DFT), the semilocal DFT (LYP) correlation E_C(DFT), the MP2 correlation ($E2$), and the zero-point vibrational energy E_{ZPVE}. Summing the contributing components gives the total atomization energy:

$$\mathrm{TAE} = \Delta E_{TVJN} + \Delta E_X^{HF} + \Delta E_X^{DFT} + \Delta E_C^{DFT} + \Delta E2 + \Delta E_{ZPVE} \quad (5)$$

where

$$\Delta E = \sum E_{atoms} - E_{molecule}$$

The decrease in the TAE as the basis set size is reduced is apparent for both the Dunning and Pople basis sets. Although the change in contributions when the basis set size is decreased for many of the components is complex when viewed across the three prototypical molecules, some important trends are clear. The first is the consistent decline in the contribution of MP2 correlation ($\Delta E2$) to the total atomization energy when smaller basis sets are employed. As is the case for standard MP2, when smaller basis sets are used with B2-PLYP they are no longer able to recover a significant proportion of the correlation energy. In contrast, the contribution of the correlation energy from the DFT portion of the B2-PLYP method (i.e., LYP) remains almost perfectly constant, indicating that basis set convergence of the DFT portion (ΔE_C(DFT)) of the correlation energy has effectively already been achieved at the double-ζ level.

Making up for this inadequate MP2 correlation with small basis sets through reparametrization of the B2-PLYP method is difficult, as evidenced by the poor results for the B2-PLYP methods in Table 3, even after they have been reoptimized for smaller basis sets. While a worthwhile improvement in performance is gained after reparametrization for B2-PLYP when used with triple-ζ or larger basis sets (MAD lowerings of between 0.6 and 5.5 kJ mol^{-1}), the improvements for the smaller basis sets accompanying optimization of the methods are not sufficient to warrant their general use. It has been suggested[12] that an increase in the MP2 correlation parameter (a_C) would be required to compensate for the effects of small basis sets, but a small *decrease* in a_C is actually observed here in general under those conditions. The problem with trying to overcome the observed lack of MP2 correlation by increasing a_C is associated with how the DHDFT procedures are defined (refer eq 1). As the coefficients for MP2 correlation (a_C) and DFT correlation (1 −

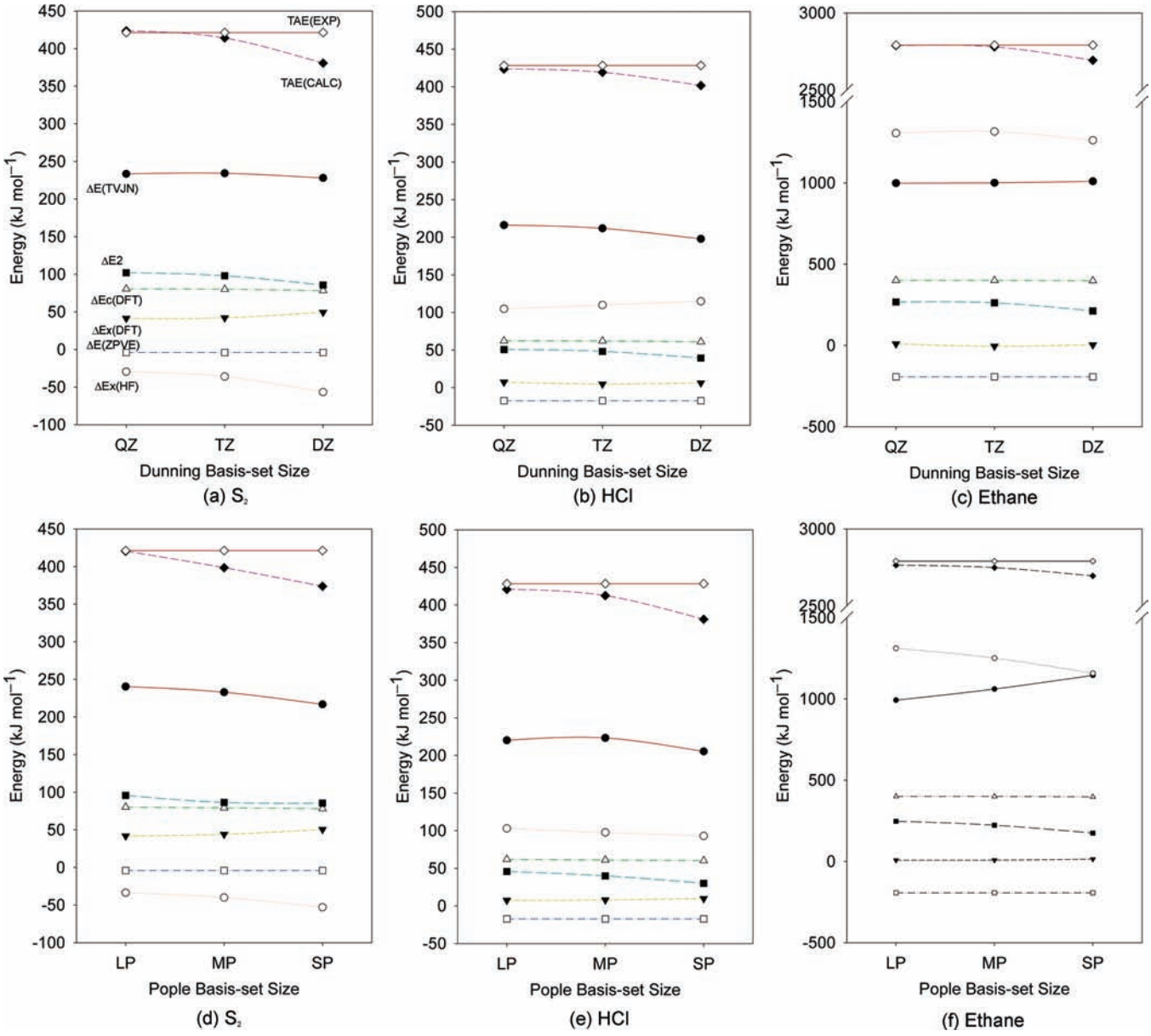

Figure 5. Effect of decreasing the size of both Dunning and Pople basis sets on the contributions of the various energy components toward the total atomization energy (TAE) for S_2 (a) and (d), HCl (b) and (e), and ethane (c) and (f). B2-PLYP parameters are constant at 62% Hartree−Fock exchange and 35% MP2 correlation. QZ = cc-pVQZ, TZ = cc-pVTZ, DZ = cc-pVDZ, LP = 6-311+G(3df,2p), MP = 6-31+G(2d,p), SP = 6-31G(d). Components: TAE(EXP) (◇); TAE(CALC) (◆); Δ*E*(TVJN) (●); Δ*E*2 (■); ΔE_C(DFT) (△); ΔE_X(DFT) (▼); Δ*E*(ZPVE) (□); ΔE_X(HF) (○).

a_C) are coupled, any attempt to increase the amount of MP2 correlation by increasing a_C will be offset somewhat by the decrease in DFT correlation. This offset is dependent on the relative contributions of E_C^{DFT} and *E*2 to the TAE, but on inspection of Figure 5 it can be seen that they are quite similar, so that the offset would also be expected to be similar. The movement in the TAE on changing the a_C parameter is complicated further by the reliance of *E*2 on the KS orbitals, which themselves are solved self-consistently depending on the contribution from E_C^{DFT}! From the present results, it appears that a reduction in overall HF exchange may be more important than the proportion of MP2 correlation in correcting the problem resulting from basis-set-size deficiency. Decreasing the amount of HF exchange admixture leads to a narrowing of the orbital gap (in eq 3), and this results in an increase in the amount of MP2 correlation.[8] This seems to work to some degree, although decoupling the MP2 and DFT correlation constants may provide a more appropriate solution to this problem.

3.3. Performance of the Optimized B2-PLYP Methods for the G3/05 Test Set. Each of the basis-set-optimized double-hybrid DFT procedures described previously were tested for their performance for the full G3/05 test set. The reparametrized UB2-PLYP(62,35) method with the cc-pVQZ basis set performs very well, with the overall MAD of 9.9 kJ mol^{-1} (Table 4) performing slightly better than the original (U)B2-PLYP method (i.e., 10.5 kJ mol^{-1}), even though in the present case basis sets containing tight-core functions were not used. The improvement in performance across all categories in the G3/05 test set (with the exception of proton affinities) is primarily due to the change of basis set from QZV3P to cc-pVQZ. Also encouraging is the excellent performance of the method for reaction types separate from the heats of formation for which it was parametrized.

The reparametrized ROB2-PLYP(59,28) method shows a slightly superior performance when compared with UB2-PLYP(62,35) for the G3/05 test set. The overall MAD of 9.1 kJ mol^{-1} represents a slight improvement on the unrestricted

TABLE 4: Performance of the Parameter-Optimized ROB2-PLYP Methods and Influence of the s_6 Scaling Parameter on Components of the G3/05 Test Set[a,b]

		EA		IE		PA		HB		ΔH_f		
basis set	s_6	MAD	MD	MAD	MD	MAD	MD	MAD	MD	MAD	MD	overall MAD
cc-pVQZ[c]		6.3	0.3	9.4	−4.6	3.5	−1.8	2.1	0.6	11.3	0.9	9.9
cc-pVQZ		5.7	−0.3	9.3	−4.7	3.5	−1.3	2.1	0.8	10.2	2.2	9.1
cc-pVTZ		5.8	0.3	11.2	−8.2	5.7	1.7	2.2	−0.4	13.9	4.1	11.8
cc-pVDZ		13.8	10.2	30.3	−28.3	15.0	9.1	2.4	2.0	59.6	33.0	44.8
6-311+G(3df,2p)		6.2	−2.9	10.2	−5.6	5.5	−5.1	2.2	0.5	15.8	6.6	12.8
6-31+G(2d,p)		7.1	−2.1	15.5	−11.8	6.4	−5.8	1.9	1.0	26.9	15.9	20.8
6-31G(d)		11.1	1.0	37.4	−32.2	21.5	3.5	4.5	−2.9	45.6	18.5	37.8
cc-pVQZ[c]	0.30[d]	6.2	0.4	9.5	−4.6	3.5	−1.4	2.4	−1.1	11.0	−2.7	9.7
cc-pVQZ	0.40[d]	5.7	−0.3	9.3	−4.7	3.6	−0.8	2.6	−1.4	10.9	−2.5	9.5
cc-pVQZ[b]	0.20[e]	6.2	0.3	9.5	−4.6	3.5	−1.5	2.3	−0.5	10.9	−1.5	9.6
cc-pVQZ	0.20[e]	5.7	−0.3	9.3	−4.7	3.6	−1.0	2.3	−0.3	9.8	−0.1	8.9

[a] All energies are in kJ mol^{-1}. [b] All methods are restricted (ROB2-PLYP) unless otherwise noted and use the basis-set optimized parameters listed in Table 3. [c] UB2-PLYP(62,35). [d] Optimized values using the S22 test set. [e] Optimized value using the G3/05 test set. EA = electron affinities (63), IE = ionization energies (105), PA = proton affinities (10), HB = hydrogen-bond energies (6), and ΔH_f = heats of formation (271).

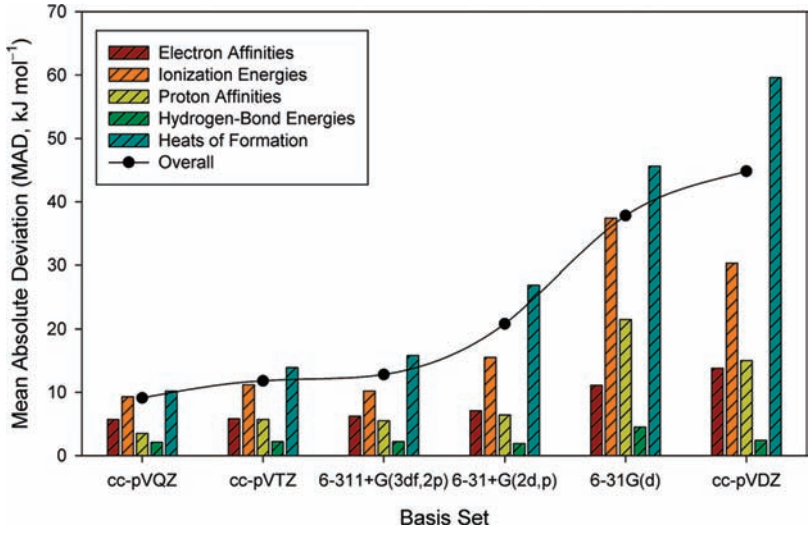

Figure 6. Effect of basis set size on the mean absolute deviation (MAD) from experiment of the parameter-optimized ROB2-PLYP(X,C) methods on the various components of the G3/05 test set. Note that diffuse functions are included in all basis sets for the calculation of electron affinities and hydrogen-bond energies; see text.

method (MAD = 9.9 kJ mol^{-1}) and results from an equal or better performance on each of the subsets of the G3/05 test set. ROB2-PLYP(59,28) performs better than UB2-PLYP(62,35) for most of the situations where calculations on open-shell species are involved, i.e., for electron affinities, ionization energies and heats of formation.

The overall and individual subset performance of each basis-set-optimized ROB2-PLYP(X,C) method for the G3/05 test set is shown graphically in Figure 6. Mirroring the results obtained for the G2/97 heats of formation set, errors with the optimized ROB2-PLYP(X,C) methods become significant once the basis set is reduced to below triple-ζ quality. For the smaller basis sets, much of the overall error is attributed to larger errors in the ionization energy and heats of formation sets. All basis sets perform reasonably well for electron affinities and hydrogen-bond energies, although this may be partly due to the additional diffuse functions used in the calculation of these quantities (refer to Theoretical Methods).

3.4. Incorporation of Dispersion Correction into the Optimized ROB2-PLYP and UB2-PLYP Methods. In an effort to improve the UB2-PLYP(62,35)/cc-pVQZ and ROB2-PLYP(59,28)/cc-pVQZ model chemistries even further, we have examined the effect of an empirical dispersion correction (DFT-D), as previously proposed by Grimme.[34,35] This type of correction was found to greatly improve the performance of both standard[35] and double-hybrid[34] DFT procedures for van der Waals complexes. Because double-hybrid DFT procedures are already capable of partially recovering dispersion via their $E2$ component,[15,34] an empirical scaling (damping) factor (s_6) is typically employed that has been found to be dependent on the amount of $E2$ admixture in the DHDFT procedures.[12]

Following the method used by both Grimme[35] and Martin,[12] we have optimized the dispersion scaling factor using the S22 benchmark set of interaction energies of Hobza and co-workers,[45] which includes both large and small dispersive and hydrogen-bonded systems. The same aug-cc-pVTZ basis set used in Grimme's original approach[34] was employed for optimization of the s_6 values for both the UB2-PLYP(62,35)-D and ROB2-PLYP(59,28)-D methods. The MAD from high-level theory for the S22 set with (U/RO)B2-PLYP-D is given as a function of the s_6 parameter in Figure 7 and Table 6. A half-counterpoise-correction (HCP) was applied to the interaction energies as it represents a suitable compromise between a full counterpoise correction (CP) and a non-counterpoise-corrected approach.[34] The optimum s_6 values that minimize the MAD for the S22 set when the half-counterpoise correction is included

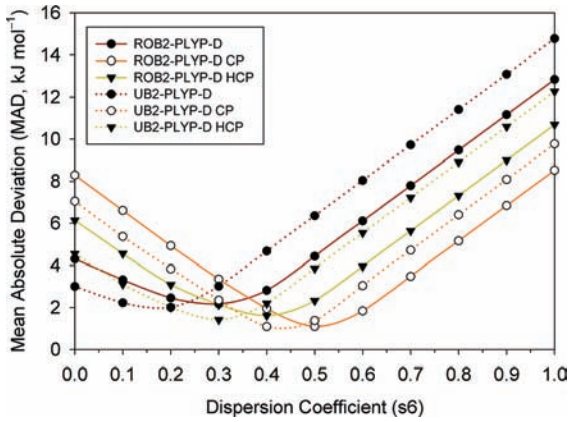

Figure 7. Effect of the s_6 dispersion coefficient on the mean absolute deviation (MAD) from high-level theoretical values for the interaction energies in the S22 test set using the ROB2-PLYP(59,28) and UB2-PLYP(62,35) methods. (U/RO)B2-PLYP-D and (U/RO)B2PLYP-D-CP refer to the uncorrected and counterpoise-corrected energies, respectively, while (U/RO)B2-PLYP-D-HCP is their average; i.e., it includes half the counterpoise correction.

are found to be 0.40 for ROB2-PLYP(59,28)-D HCP and 0.30 for UB2-PLYP(62,35)-D HCP after rounding to the nearest 0.05. The larger value obtained for the restricted method is not surprising as this method contains only 28% MP2 correlation, compared with 35% in the unrestricted method, which contributes significantly toward taking care of dispersive effects. The dispersion correction leads to an improvement in the MAD for the S22 set from 4.6 to 1.4 kJ mol^{-1} for UB2-PLYP(62,35)-D HCP and from 6.1 to 1.6 kJ mol^{-1} for ROB2-PLYP(59,28)-D HCP.

When applied to the G3/05 test set (Table 4), incorporation of the new dispersion correction leads to a decrease in the overall MAD from 9.9 to 9.7 kJ mol^{-1} for UB2-PLYP-D, while the MAD for the ROB2-PLYP-D method *increases* from 9.1 to 9.5 kJ mol^{-1}. The increase in the MAD for ROB2-PLYP-D is primarily due to the decline in performance for the heats of formation within the G3/05 set where an increase in the MAD from 10.2 to 10.9 kJ mol^{-1} is observed. The source of this error can be traced further by subdividing the G3/05 heats of formation into the G2/97 heats of formation set (148 molecules), the G3/99 supplement to the G2/97 heats of formation (75) (referred to as the G3/99 supplementary set), and the G3/05 supplement to the G3/99 heats of formation (48) (referred to as the G3/05 supplementary set). The increase in MAD for the ROB2-PLYP(59,28)-D method is found to be primarily due to a 2.6 kJ mol^{-1} increase in the G3/05 ΔH_f supplementary set on adding the scaled dispersion function (Table 5). Interestingly, the UB2-PLYP(62,35)-D method also shows an increase in the MAD for this subset on the addition of the dispersion function, although it is not as severe as that for the restricted form. This difference is likely to be a consequence of the smaller dispersion coefficient used in the unrestricted method. The overall reduction in MAD for the G2/97 and G3/99 ΔH_f supplementary sets on including dispersion is still good for the unrestricted method, with these results supporting the 2.9 kJ mol^{-1} improvement previously reported.[34]

The G3/99 ΔH_f supplementary set is primarily composed of large unsubstituted and substituted hydrocarbons where a dispersion correction is expected to make an important contribution. The species that comprise the G3/05 ΔH_f supplementary set, on the other hand, are primarily small to medium-sized inorganic species where dispersion is expected to have a more moderate effect. The increase in error when dispersion is applied to the ROB2-PLYP(59,28) method is not so much the fault of the dispersion function itself (or the dispersion scaling factor). Rather, it is due to the population skew present in the heats of formation error distribution before dispersion is applied, which results from the choice of the original a_X and a_C parameters.

TABLE 5: Influence of the B2-PLYP-D s_6 Dispersion Coefficient on the Mean Absolute Deviations (MADs) and Mean Deviations (MDs) from Experimental Values for Components of the G3/05 Heats of Formation Test Set[a]

		G2/97 ΔH_f set (148)		G3/99 ΔH_f supplementary set (75)		G3/05 ΔH_f supplementary set (48)	
method[b]	s_6	MAD	MD	MAD	MD	MAD	MD
cc-pVQZ[c]	0.00	7.4	−0.1	15.6	5.4	16.4	−3.3
cc-pVQZ	0.00	6.6	1	14.6	7.1	14.7	−1.6
cc-pVQZ[c]	0.30[d]	7.3	−1.9	13.5	−2.6	18.5	−5.2
cc-pVQZ	0.40[d]	7.2	−1.4	14.1	−3.6	17.3	−4.1
cc-pVQZ[c]	0.20[e]	7.2	−1.3	13.7	0.1	17.8	−4.6
cc-pVQZ	0.20[e]	6.6	−0.2	12.3	1.7	16.0	−2.9

[a] All energies are in kJ mol^{-1}. [b] All methods are restricted [ROB2-PLYP(59,28)] unless otherwise noted. [c] UB2-PLYP(62,35). [d] Optimum dispersion coefficient calculated using the S22 test set. [e] Optimum dispersion coefficient calculated using the full G3/05 test set.

TABLE 6: Influence of the s_6 Dispersion Coefficient on the Mean Absolute Deviations from High-Level Theoretical Values of Interaction Energies for ROB2-PLYP(59,28) and UB2-PLYP(62,35)-D for the S22 Test Set[a]

s_6	ROB2-PLYP(59,28)	ROB2-PLYP-D-CP	ROB2-PLYP-D-HCP	UB2-PLYP(62,35)	UB2-PLYP-D-CP	UB2PLYP-D-HCP
0.0	4.3	8.3	6.1	3.0	7.1	4.6
0.1	3.3	6.6	4.6	2.2	5.4	3.1
0.2	2.5	4.9	3.1	2.0	3.8	2.0
0.3	2.2	3.3	2.1	3.0	2.4	1.4
0.4	2.8	1.9	1.6	4.7	1.1	2.2
0.5	4.4	1.1	2.3	6.4	1.4	3.9
0.6	6.1	1.8	4.0	8.0	3.0	5.5
0.7	7.8	3.5	5.6	9.7	4.7	7.2
0.8	9.5	5.2	7.3	11.4	6.4	8.9
0.9	11.2	6.8	9.0	13.1	8.1	10.6
1.0	12.8	8.5	10.7	14.8	9.8	12.3

[a] All energies are in kJ mol^{-1}.

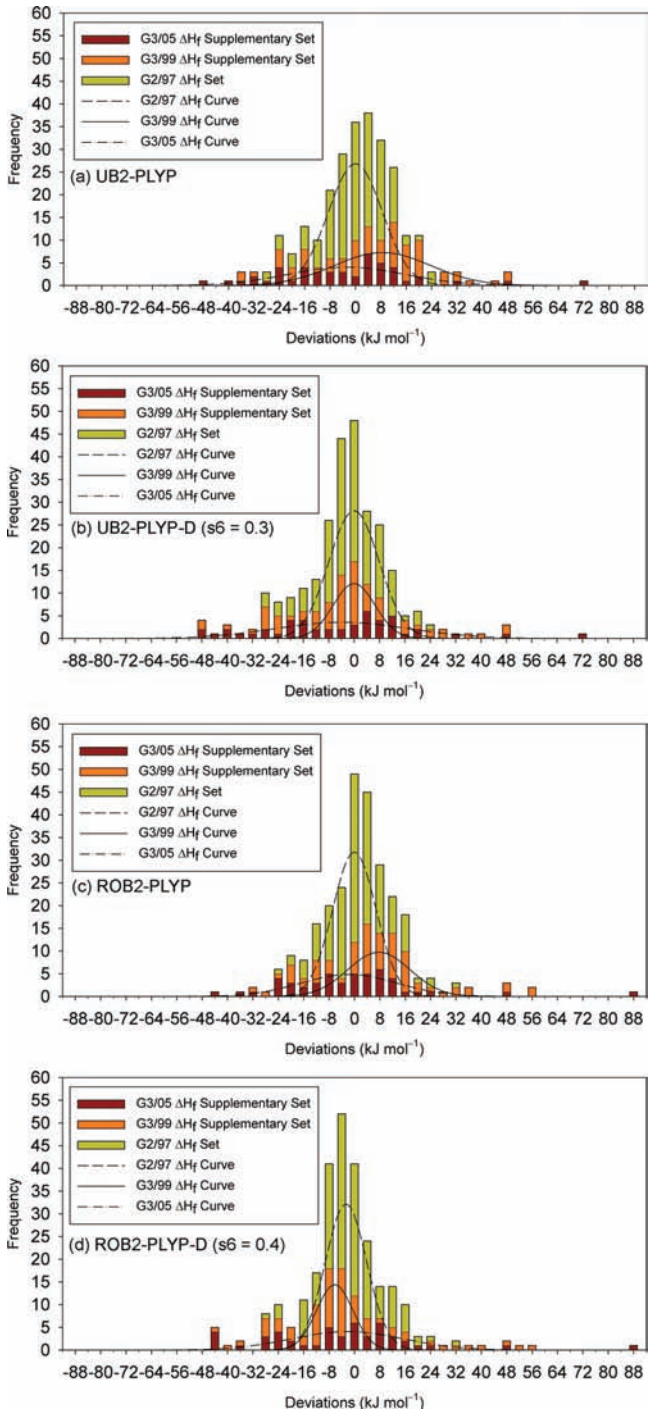

Figure 8. Effect of including the S22-optimized scaling parameter (s_6) as part of the UB2-PLYP(62,35) and ROB2-PLYP(59,28) methods on the distribution of deviations from experimental values for the G3/05 heats of formation test set. The G3/05 heats of formation set is divided to show the G2/97 ΔH_f (yellow bars), the G3/99 ΔH_f supplementary set (orange bars), and the G3/05 ΔH_f supplementary set (red bars). Each vertical bar represents deviations in a 4 kJ mol^{-1} range.

Figure 8 shows distribution curves fitted to the subsets comprising the G3/05 heat of formation set before and after the dispersion correction is applied. By design, the addition of the dispersion correction shifts the skew of the populations to the left, with a more dramatic shift shown for those populations containing large molecules (i.e., the G3/99 ΔH_f supplementary set) or for methods where a larger dispersion scaling factor is applied (i.e., ROB2-PLYP(59,28)-D). The action of the included

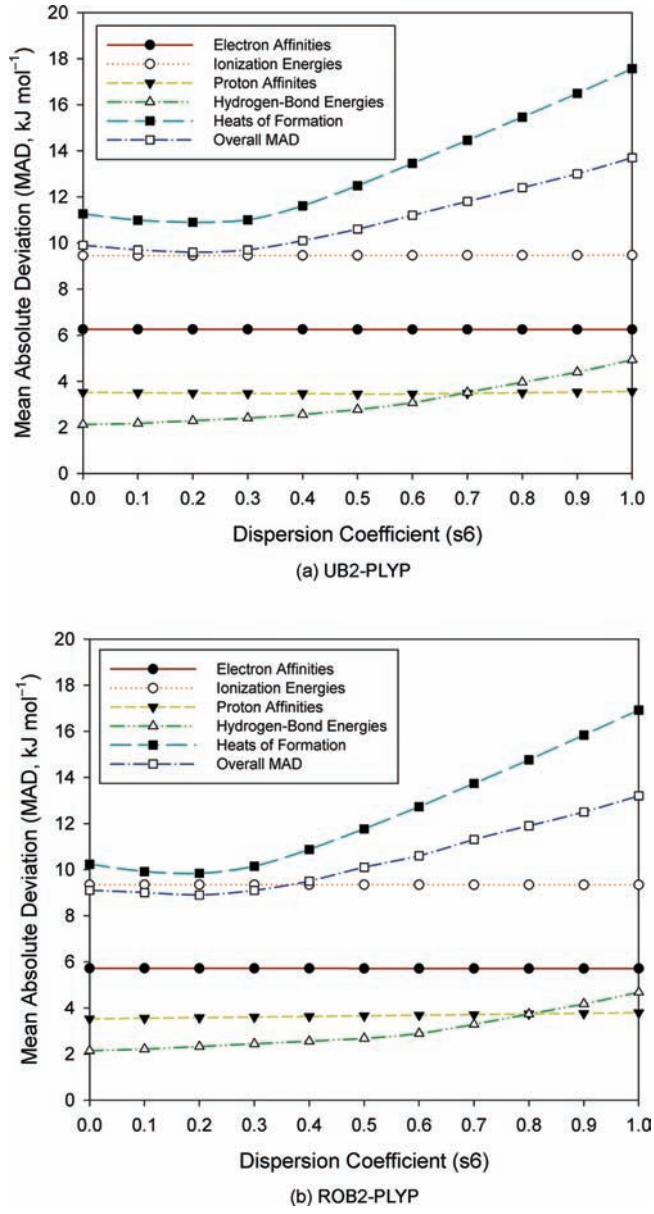

Figure 9. Effect of the s_6 scaling parameter on the mean absolute deviation from experimental values for the full G3/05 test set when using the (a) UB2-PLYP and (b) ROB2-PLYP methods.

dispersion function is to correct the right-skew of the G3/99 ΔH_f supplementary set, but the unfortunate consequence is an increase in the left-skew of both the G3/05 ΔH_f supplementary set and the G2/97 ΔH_f set, ultimately increasing their MADs. Clearly, the addition of a dispersion function to produce a general purpose double-hybrid DFT procedure without the reoptimization of the HF exchange and MP2 correlation coefficients can give mixed results. This is interesting given that it might have been expected that no refit would be required for the nondispersion part because the parameters were derived on relatively small systems.[34]

The results of the re-evaluation of the s_6 scaling parameters using the entire G3/05 set while the optimized DHDF parameters are kept constant are shown in Figure 9. Optimum values for the s_6 scaling parameter for the UB2-PLYP(62,35) and ROB2-PLYP(59,28) methods are both found to be 0.2. The improvement in the overall MAD for heats of formation is a modest 0.4 kJ mol^{-1} for both UB2-PLYP and ROB2-PLYP, resulting in an overall decrease in MAD across the entire G3/05 test set

of 0.3 and 0.2 kJ mol^{-1}, respectively (Table 4). On balance, however, we would favor the use of the s_6 parameters optimized for the S22 set, since this is likely to better cope with the description of van der Waals interactions.

4. Conclusions

In this study we have assessed the performance of the parameter-optimized versions of the restricted-open-shell form of the double-hybrid density functional theory (DHDFT) B2-PLYP procedure against that of its unrestricted counterpart for the 455 energies that comprise the G3/05 test set. In addition, we have investigated the influence of basis set on both the parametrization and performance of the ROB2-PLYP methods and have examined their further improvement through augmentation with a long-range dispersion function. We have reached the following conclusions:

(1) Optimization of the two empirical parameters of the UB2-PLYP(X,C) procedure using the G2/97 heats of formation test set with the cc-pVQZ basis set results in Hartree−Fock exchange and MP2 correlation scaling values of $a_X = 62\%$ and $a_C = 35\%$, respectively. For the ROB2-PLYP(X,C) procedure, the corresponding optimized parameters are $a_X = 59\%$ and $a_C = 28\%$.

(2) When tested against the entire G3/05 test set, the UB2-PLYP(62,35)/cc-pVQZ model chemistry gives a mean absolute deviation (MAD) from experiment of 9.9 kJ mol^{-1}. ROB2-PLYP(59,28)/cc-pVQZ gives a slightly better MAD from experiment of 9.1 kJ mol^{-1}. The restricted form of the method performs better in the areas where calculation of open-shell species is involved, i.e., electron affinities, ionization energies, and heats of formation. This suggests that spin contamination has a minor, but measurable effect on the performance of the unrestricted DHDFT procedures.

(3) It is essential to use optimized parameters for ROB2-PLYP(X,C) to gain full benefit from the improved performance. For example, the MAD values for the G2/97 test set are 13.5 and 12.2 kJ mol^{-1}, respectively, for ROB2-PLYP(62,35) and ROB2-PLYP(53,27) compared with just 6.6 kJ mol^{-1} for (the optimized) ROB2-PLYP(59,28).

(4) The inclusion of a spin−orbit correction in optimizing the DHDFT parameters results in a small change in the optimum parameters but also in a deterioration in performance for both the unrestricted- and restricted-open-shell methods.

(5) Reoptimization of the ROB2-PLYP parameters using the G2/97 heats of formation test set with basis sets smaller than cc-pVQZ results in significant changes in both the optimized parameters and the performance of the method. In order of increasing MAD from experiment, the optimized parameters and MAD values are cc-pVQZ(59,28) (MAD = 6.6 kJ mol^{-1}), cc-pVTZ(60,32) (MAD = 9.5 kJ mol^{-1}), 6-311+G(3df,2p)(55,27) (MAD = 11.2 kJ mol^{-1}), 6-31+G(2d,p)(53,25) (MAD = 18.8 kJ mol^{-1}), 6-31G(d)(5,0) (MAD = 32.2 kJ mol^{-1}), and cc-pVDZ(28,22) (MAD = 47.2 kJ mol^{-1}). The enhanced basis-set dependence compared with standard DFT procedures reflects the incorporation of an MP2 component. As the contributions of DFT correlation and MP2 correlation are inherently linked through the a_C parameter in DHDFT procedures, a reduction in overall Hartree−Fock exchange appears to be more important than increasing the amount of MP2 correlation when trying to rectify the consequences stemming from the basis-set-size deficiency. Reoptimization of the (59,28) parameters gives an improvement in the MAD of between 0 and 41 kJ mol^{-1} for the G2/97 heats of formation set for the various basis sets. This suggests that at least some of the deficiency of DHDFT procedures caused by the use of smaller basis sets can be overcome through reparametrization. However, in the cases where the basis set is less than triple-ζ quality, the improvements made on reoptimizing the (double-hybrid) ROB2-PLYP parameters are not sufficient to warrant their general use, and the (single-hybrid) ROB3-LYP procedure actually shows superior performance.

(6) The empirical dispersion scaling coefficient (s_6) has been calculated for the ROB2-PLYP(59,28)-D procedure by minimizing the MAD for the S22 test set. The optimum s_6 value is found to be 0.40 for ROB2-PLYP(59,28)-D HCP, and this leads to an improvement in the MAD for the S22 set from 6.1 to 1.6 kJ mol^{-1}. Performance of the dispersion-incorporated ROB2-PLYP(59,28)-D method for the G3/05 test set, however, deteriorates from an MAD of 9.1 kJ mol^{-1} (without dispersion, i.e., $s_6 = 0$) to 9.5 kJ mol^{-1} (with $s_6 = 0.40$), primarily due to an increase of 2.6 kJ mol^{-1} in the MAD for the G3/05 heats of formation supplementary set. While the addition of dispersion greatly improves the performance for large organic molecules, the small- to medium-sized inorganic molecules in the G3/05 heats of formation supplementary set are handled more poorly. Nevertheless, the significant improvements for species where a satisfactory description of dispersion is more important, makes the ROB2-PLYP-D procedure an attractive choice.

Acknowledgment. We gratefully acknowledge the award of a Henry Bertie Florence Mabel Gritton Scholarship (to A.S.M.), the award of a Fonds der Chemischen Industrie Scholarship (to L.G.), the award of an Australian Professorial Fellowship and funding from the ARC Centre of Excellence for Free Radical Chemistry and Biotechnology (to L.R.), and generous allocations of computer time from the NCI National Facility and the Australian Centre for Advanced Computing and Communications (ac3). We thank Professor Jan Martin for providing us with preprints of refs 12a and 12b.

Supporting Information Available: Calculated total energies for atoms and molecules from the G2/97 heats of formation set and their deviation from experimental values for UB2-PLYP/cc-pVQZ (Table S1), ROB2-PLYP/cc-pVQZ (Table S2), ROB2-PLYP/cc-pVTZ (Table S3), ROB2-PLYP/cc-pVDZ (Table S4), ROB2-PLYP/6-311+G(3df,2p) (Table S5), ROB2-PLYP/6-31+G(2d,p) (Table S6), and ROB2-PLYP/6-31G(d) (Table S7). Calculated total energies for atoms and molecules from the G2/97 heats of formation set and their deviation from experimental values for the ROB-LYP and ROB3-LYP model chemistries (Table S8). Calculated total energies, and contributions to the total atomization energy for S_2, HCl and ethane (Table S9). Calculated total energies, unscaled dispersion corrections and deviations from experiment for the subsets of the G3/05 test set with the UB2-PLYP(62,35)/cc-pVQZ, ROB2-PLYP(59,28)/cc-pVQZ, ROB2-PLYP(60,32)/cc-pVTZ, ROB2-PLYP(28,22)/cc-pVDZ, ROB2-PLYP(55,27)/6-311+G(3df,2p), ROB2-PLYP(53,25)/6-31+G(2d,p), ROB2-PLYP(5,0)/6-31G(d) model chemistries (Table S10). Interaction energies, counterpoise corrections and dispersion contributions to the S22 test set (Table S11). This material is available free of charge via the Internet at http://pubs.acs.org.

References and Notes

(1) (a) Pople, J. A.; Head-Gordon, M.; Fox, D. J.; Raghavachari, K.; Curtiss, L. A. *J. Chem. Phys.* **1989**, *90*, 5622–5629. (b) Curtiss, L. A.; Jones, C.; Trucks, G. W.; Raghavachari, K.; Pople, J. A. *J. Chem. Phys.* **1990**, *93*, 2537–2545. (c) Curtiss, L. A.; Raghavachari, K.; Trucks, G. W.; Pople, J. A. *J. Chem. Phys.* **1991**, *94*, 7221–7230. (d) Curtiss, L. A.; Raghavachari,

K.; Pople, J. A. *J. Chem. Phys.* **1993**, *98*, 1293–1298. (e) Curtiss, L. A.; McGrath, M. P.; Blaudeau, J. P.; Davis, N. E.; Binning, R. C.; Radom, L. *J. Chem. Phys.* **1995**, *103*, 6104–6113. (f) Curtiss, L. A.; Raghavachari, K.; Redfern, P. C.; Rassolov, V.; Pople, J. A. *J. Chem. Phys.* **1998**, *109*, 7764–7776. (g) Curtiss, L. A.; Redfern, P. C.; Raghavachari, K.; Rassolov, V.; Pople, J. A. *J. Chem. Phys.* **1999**, *110*, 4703–4709. (h) Baboul, A. G.; Curtiss, L. A.; Redfern, P. C.; Raghavachari, K. *J. Chem. Phys.* **1999**, *110*, 7650–7657. (i) Curtiss, L. A.; Redfern, P. C.; Raghavachari, K.; Pople, J. A. *J. Chem. Phys.* **2001**, *114*, 108–117. (j) Curtiss, L. A.; Redfern, P. C.; Raghavachari, K. *J. Chem. Phys.* **2007**, *126*, 084108. (k) Curtiss, L. A.; Redfern, P. C.; Raghavachari, K. *J. Chem. Phys.* **2007**, *127*, 124105.

(2) (a) Ochterski, J. W.; Petersson, G. A.; Montgomery, J. A. *J. Chem. Phys.* **1996**, *104*, 2598–2619. (b) Montgomery, J. A.; Frisch, M. J.; Ochterski, J. W.; Petersson, G. A. *J. Chem. Phys.* **1999**, *110*, 2822–2827. (c) Montgomery, J. A.; Frisch, M. J.; Ochterski, J. W.; Petersson, G. A. *J. Chem. Phys.* **2000**, *112*, 6532–6542.

(3) (a) Martin, J. M. L.; de Oliveira, G. *J. Chem. Phys.* **1999**, *111*, 1843–1856. (b) Boese, A. D.; Oren, M.; Atasoylu, O.; Martin, J. M. L.; Kallay, M.; Gauss, J. *J. Chem. Phys.* **2004**, *120*, 4129–4141. (c) Karton, A.; Rabinovich, E.; Martin, J. M. L.; Ruscic, B. *J. Chem. Phys.* **2006**, *125*, 144108.

(4) Schwabe, T.; Grimme, S. *Acc. Chem. Res.* **2008**, *41*, 569–579.

(5) Cremer, D. *Mol. Phys.* **2001**, *99*, 1899–1940.

(6) Koch, W.; Holthausen, M. C. *A Chemist's Guide to Density Functional Theory*, 2nd ed.; Wiley-VCH: Weinheim, 2002.

(7) Perdew, J. P.; Ruzsinszky, A.; Tao, J. M.; Staroverov, V. N.; Scuseria, G. E.; Csonka, G. I. *J. Chem. Phys.* **2005**, *123*, 062201.

(8) Grimme, S. *J. Chem. Phys.* **2006**, *124*, 034108.

(9) Schwabe, T.; Grimme, S. *Phys. Chem. Chem. Phys.* **2006**, *8*, 4398–4401.

(10) (a) Becke, A. D. *Phys. Rev. A* **1988**, *38*, 3098–3100. (b) Becke, A. D. *J. Chem. Phys.* **1993**, *98*, 5648–5652. (c) Lee, C.; Yang, W.; Parr, R. G. *Phys. Rev. B* **1988**, *37*, 785–789. (d) Stephens, P. J.; Devlin, F. J.; Chablowski, C. F.; Frisch, M. J. *J. Phys. Chem.* **1994**, *98*, 11623–11627.

(11) (a) Gorling, A.; Levy, M. *Phys. Rev. B* **1993**, *47*, 13105–13113. (b) Gorling, A.; Levy, M. *Phys. Rev. A* **1994**, *50*, 196–204.

(12) (a) Tarnopolsky, A.; Karton, A.; Sertchook, R.; Vuzman, D.; Martin, J. M. L. *J. Phys. Chem. A* **2008**, *112*, 3–8. (b) Karton, A.; Tarnopolsky, A.; Lamere, J.-F.; Schatz, G. C.; Martin, J. M. L. *J. Phys. Chem. A* **2008**, *112*, 12868–12886.

(13) (a) Vahtras, O.; Almlof, J.; Feyereisen, M. W. *Chem. Phys. Lett.* **1993**, *213*, 514–518. (b) Weigend, F.; Haser, M. *Theor. Chem. Acc.* **1997**, *97*, 331–340. (c) Kendall, R. A.; Früchtl, H. A. *Theor. Chem. Acc.* **1997**, *97*, 158–163.

(14) Grimme, S.; Steinmetz, M.; Korth, M. *J. Org. Chem.* **2007**, *72*, 2118–2126.

(15) Benighaus, T.; DiStasio, R. A.; Lochan, R. C.; Chai, J. D.; Head-Gordon, M. *J. Phys. Chem. A* **2008**, *112*, 2702–2712.

(16) Adamo, C.; Barone, V. *J. Chem. Phys.* **1998**, *108*, 664–675.

(17) (a) Menon, A. S.; Wood, G. P. F.; Moran, D.; Radom, L. *J. Phys. Chem. A* **2007**, *111*, 13638–13644. (b) Menon, A. S.; Wood, G. P. F.; Moran, D.; Radom, L. *J. Phys. Chem. A* **2008**, *112*, 5554–5554.

(18) (a) Grimme, S.; Neese, F. *J. Chem. Phys.* **2007**, *127*, 154116. (b) Goerijk, L.; Moellman, J.; Grimme, S. *Phys. Chem. Chem. Phys.* **2009**, *11*, 4611.

(19) Goerigk, L.; Grimme, S. *J. Phys. Chem. A* **2009**, *113*, 767–776.

(20) Piacenza, M.; Hyla-Kryspin, I.; Grimme, S. *J. Comput. Chem.* **2007**, *28*, 2275–2285.

(21) Neese, F.; Schwabe, T.; Grimme, S. *J. Chem. Phys.* **2007**, *126*, 124115.

(22) Tozer, D. J.; Handy, N. C.; Amos, R. D.; Pople, J. A.; Nobes, R. H.; Xie, Y. M.; Schaefer, H. F. *Mol. Phys.* **1993**, *79*, 777–793.

(23) Henry, D. J.; Sullivan, M. B.; Radom, L. *J. Chem. Phys.* **2003**, *118*, 4849–4860.

(24) Mayer, P. M.; Parkinson, C. J.; Smith, D. M.; Radom, L. *J. Chem. Phys.* **1998**, *108*, 604–615.

(25) Wood, G. P. F.; Radom, L.; Petersson, G. A.; Barnes, E. C.; Frisch, M. J.; Montgomery, J. A. *J. Chem. Phys.* **2006**, *125*, 094106.

(26) Grafenstein, J.; Hjerpe, A. M.; Kraka, E.; Cremer, D. *J. Phys. Chem. A* **2000**, *104*, 1748–1761.

(27) Pople, J. A.; Gill, P. M. W.; Handy, N. C. *Int. J. Quantum Chem.* **1995**, *56*, 303–305.

(28) Cohen, A. J.; Tozer, D. J.; Handy, N. C. *J. Chem. Phys.* **2007**, *126*, 214104.

(29) Menon, A. S.; Radom, L. *J. Phys. Chem. A* **2008**, *112*, 13225–13230.

(30) (a) Beran, G. J. O.; Gwaltney, S. R.; Head-Gordon, M. *Phys. Chem. Chem. Phys.* **2003**, *5*, 2488–2493. (b) Bartlett, R. J.; Lotrich, V. F.; Schweigert, I. V. *J. Chem. Phys.* **2005**, *123*, 062205.

(31) (a) Grimme, S. *Chem. Phys. Lett.* **1996**, *259*, 128–137. (b) Grimme, S.; Waletzke, M. *J. Chem. Phys.* **1999**, *111*, 5645–5655. (c) Bour, P. *Chem. Phys. Lett.* **2001**, *345*, 331–337.

(32) (a) Bour, P. *J. Comput. Chem.* **2000**, *21*, 8–16. (b) Mori-Sanchez, P.; Wu, Q.; Yang, W. T. *J. Chem. Phys.* **2005**, *123*, 062204.

(33) (a) Pratt, D. A.; Wright, J. S.; Ingold, K. U. *J. Am. Chem. Soc.* **1999**, *121*, 4877–4882. (b) DiLabio, G. A.; Pratt, D. A.; LoFaro, A. D.; Wright, J. S. *J. Phys. Chem. A* **1999**, *103*, 1653–1661. (c) Wood, G. P. F.; Henry, D. J.; Radom, L. *J. Phys. Chem. A* **2003**, *107*, 7985–7990. (d) Gomez-Balderas, R.; Coote, M. L.; Henry, D. J.; Radom, L. *J. Phys. Chem. A* **2004**, *108*, 2874–2883.

(34) Schwabe, T.; Grimme, S. *Phys. Chem. Chem. Phys.* **2007**, *9*, 3397–3406.

(35) (a) Grimme, S. *J. Comput. Chem.* **2004**, *25*, 1463–1473. (b) Grimme, S. *J. Comput. Chem.* **2006**, *27*, 1787–1799.

(36) Schafer, A.; Huber, C.; Ahlrichs, R. *J. Chem. Phys.* **1994**, *100*, 5829–5835.

(37) Dunning, T. H. *J. Chem. Phys.* **1989**, *90*, 1007–1023.

(38) Merrick, J. P.; Moran, D.; Radom, L. *J. Phys. Chem. A* **2007**, *111*, 11683–11700.

(39) Feller, D.; Peterson, K. A. *Chem. Phys. Lett.* **2006**, *430*, 459–463.

(40) Rienstra-Kiracofe, J. C.; Tschumper, G. S.; Schaefer, H. F.; Nandi, S.; Ellison, G. B. *Chem. Rev.* **2002**, *102*, 231–282.

(41) Curtiss, L. A.; Raghavachari, K.; Redfern, P. C.; Pople, J. A. *J. Chem. Phys.* **1997**, *106*, 1063–1079.

(42) Curtiss, L. A.; Redfern, P. C.; Raghavachari, K. *J. Chem. Phys.* **2005**, *123*, 124107.

(43) Curtiss, L. A.; Raghavachari, K.; Redfern, P. C.; Pople, J. A. *J. Chem. Phys.* **2000**, *112*, 7374–7383.

(44) Nicolaides, A.; Rauk, A.; Glukhovtsev, M. N.; Radom, L. *J. Phys. Chem.* **1996**, *100*, 17460–17464.

(45) Jurecka, P.; Sponer, J.; Cerny, J.; Hobza, P. *Phys. Chem. Chem. Phys.* **2006**, *8*, 1985–1993.

(46) Boys, S. F.; Bernardi, F. *Mol. Phys.* **1970**, *19*, 553. Jansen, H. B.; Ros, P. *Chem. Phys. Lett.* **1969**, *3*, 140–143.

(47) Frisch, M. J.; Trucks, G. W.; Schlegel, H. B.; Scuseria, G. E.; Robb, M. A.; Cheeseman, J. R.; Montgomery, J. A., Jr.; Vreven, T.; Kudin, K. N.; Burant, J. C.; Millam, J. M.; Iyengar, S. S.; Tomasi, J.; Barone, V.; Mennucci, B.; Cossi, M.; Scalmani, G.; Rega, N.; Petersson, G. A.; Nakatsuji, H.; Hada, M.; Ehara, M.; Toyota, K.; Fukuda, R.; Hasegawa, J.; Ishida, M.; Nakajima, T.; Honda, Y.; Kitao, O.; Nakai, H.; Klene, M.; Li, X.; Knox, J. E.; Hratchian, H. P.; Cross, J. B.; Adamo, C.; Jaramillo, J.; Gomperts, R.; Stratmann, R. E.; Yazyev, O.; Austin, A. J.; Cammi, R.; Pomelli, C.; Ochterski, J. W.; Ayala, P. Y.; Morokuma, K.; Voth, G. A.; Salvador, P.; Dannenberg, J. J.; Zakrzewski, V. G.; Dapprich, S.; Daniels, A. D.; Strain, M. C.; Farkas, O.; Malick, D. K.; Rabuck, A. D.; Raghavachari, K.; Foresman, J. B.; Ortiz, J. V.; Cui, Q.; Baboul, A. G.; Clifford, S.; Cioslowski, J.; Stefanov, B. B.; Liu, G.; Liashenko, A.; Piskorz, P.; Komaromi, I.; Martin, R. L.; Fox, D. J.; Keith, T.; Al-Laham, M. A.; Peng, C. Y.; Nanayakkara, A.; Challacombe, M.; Gill, P. M. W.; Johnson, B.; Chen, W.; Wong, M. W.; Gonzalez, C.; Pople, J. A.; *Gussian 03*, revision B.05; Gaussian, Inc.: Pittsburgh, PA, 2003.

(48) These calculations were carried out with UB2-PLYP(62,35) because the desired energy decomposition of eq 5 does not appear to be available in Gaussian 03 for restricted-open-shell treatments.

JP9042864